Universal algebraic convergence in time of pulled fronts: the common mechanism for difference-differential and partial differential equations

UTE EBERT[1], WIM VAN SAARLOOS[2] and BERT PELETIER[3]

[1]*CWI, Postbus 94079, 1090 GB Amsterdam, The Netherlands*
[2]*Instituut–Lorentz, Universiteit Leiden, Postbus 9506, 2300 RA Leiden, The Netherlands*
[3]*Mathematical Institute, Universiteit Leiden, Postbus 9512, 2300 RA Leiden, The Netherlands*

We analyze the front structures evolving under the difference-differential equation $\partial_t C_j = -C_j + C_{j-1}^2$ from initial conditions $0 \leqslant C_j(0) \leqslant 1$ such that $C_j(0) \to 1$ as $j \to \infty$ sufficiently fast. We show that the velocity $v(t)$ of the front converges to a constant value v^* according to $v(t) = v^* - 3/(2\lambda^* t) + (3\sqrt{\pi}/2) D\lambda^*/(\lambda^{*2} Dt)^{3/2} + \mathcal{O}(1/t^2)$. Here v^*, λ^* and D are determined by the properties of the equation linearized around $C_j = 1$. The same asymptotic expression is valid for fronts in the nonlinear diffusion equation, where the values of the parameters λ^*, v^* and D are specific to the equation. The identity of methods and results for both equations is due to a common propagation mechanism of these so-called pulled fronts. This gives reasons to believe that this universal algebraic convergence actually occurs in an even larger class of equations.

1 Introduction

We consider the invasion of one homogeneous state by another in a one-dimensional system, creating a propagating front between them. The most familiar case is fronts in bistable systems, where the invading as well as invaded state are dynamically stable against small perturbations. If, on the other hand, the invaded state is unstable, one can identify two basically distinct mechanisms of propagation that depend upon further properties of the dynamical system, and apply to the evolution of all initial conditions decaying sufficiently rapidly into the unstable state. The two mechanisms are conveniently distinguished by the notion of the asymptotic front speed, v_{as}. For differential equations, this speed is defined as the large time limit of the slope $v(t)$ of level curves of the front-type solution in the (x, t)-plane. The *linear spreading velocity* v^* is defined as the asymptotic speed for the evolution equation linearized around the unstable invaded state. Since a nonlinear front never can move slower than the linear spreading speed, since otherwise the leading edge would outrun the nonlinear profile, it is clear that $v_{as} \geqslant v^*$. The distinction between the two types of fronts lies in whether v_{as} is larger than or equal to v^*. Fronts for which $v_{as} = v^*$ are sometimes referred to as *pulled*, while those for which $v_{as} > v^*$ are then called *pushed* [18, 16]. Here we will focus on pulled fronts. We will comment on

extensions of our difference-differential equation to the pushed regime in the concluding section.

Although these ideas are often phrased in different languages within different communities, they are all illustrated by the properties of solutions of the celebrated nonlinear diffusion equation

$$\partial_t \phi = \partial_x^2 \phi + f(\phi), \qquad f(\phi) = \phi - \phi^3, \tag{1.1}$$

which goes back to the work of Fisher [8] and Kolmogoroff *et al.* [13]. It is well known [8, 13, 2] that sufficiently rapidly decaying initial conditions $\phi(x, 0)$, such that $\lim_{x \to \infty} \phi(x, 0) \, e^x = 0$ lead to fronts with $v_{as} = v^* = 2$, so that fronts are indeed *pulled*.

It is the main purpose of this paper to highlight the fact that the general mechanism underlying the formation of pulled fronts extends far beyond the simple statement $v_{as} = v^*$, and is shared by a large variety of dynamical systems. In particular, we focus on the universality of the convergence towards the asymptotic front speed and shape, caused by the general dynamical mechanism of pulled front propagation.

We illustrate this observation by considering front propagation in which a stable state invades an unstable state in a differential-difference equation. The equation concerned arises in kinetic theory [24], and is given by

$$dC_j(t)/dt = -C_j(t) + C_{j-1}^2(t). \tag{1.2}$$

We stress that, although (1.2) might resemble (1.1) at first sight, the two equations describe very different types of dynamics. This is illustrated by the fact that the change of C_j depends, according to (1.2), only on C_j itself, and the variable C_{j-1} to the immediate left of it, while the nonlinear diffusion equation (1.1) is reflection symmetric in x. The origin of this asymmetric dynamics is best made clear by summarizing the derivation of (1.2) from kinetic theory.

The context is a clock model for a dilute gas of N particles with short range interactions, in which every particle carries a clock with a discrete time $k \in \mathbf{Z}$ which is advanced at every collision [24]. This happens according to the following rule: when two particles collide, they *both* reset their respective clock values, say k and ℓ, to either $k + 1$ or $\ell + 1$, whichever is the largest. Thus, if we denote the number of particles with clock value k by N_k, we obtain the following dynamical equation:

$$\frac{dN_k}{dt} = - \sum_{\ell=-\infty; \ \ell \neq k}^{\infty} R_{k,\ell} - 2R_{k,k} + 2 \sum_{\ell=-\infty}^{k-1} R_{k-1,\ell}, \tag{1.3}$$

where $R_{k,\ell}$ denotes the rate by which collisions occur between particles with clock values k and ℓ. We assume this rate to be proportional to $N_k N_\ell / N^2$ when $k \neq \ell$ and to $N_k^2/(2N^2)$ when two particles with equal clock value k collide (the fact that these rates are written as products of the variables N_k amounts to a mean field approximation in the original kinetic model). Then, writing $f_k = N_k/N$, using $f_\infty = 1$ and scaling the time appropriately, results in

$$\begin{aligned}
\frac{df_k}{dt} &= -f_k + f_{k-1}^2 + 2f_{k-1}C_{k-2}, \\
&= -f_k + C_{k-1}^2 - C_{k-2}^2,
\end{aligned} \tag{1.4}$$

where we have set

$$C_k = \sum_{\ell=-\infty}^{k} f_\ell. \tag{1.5}$$

Adding the equations for f_ℓ for all values of $\ell \leqslant k$ then yields equation (1.2).

Equation (1.2) has two constant solutions: $C_j = 0$ and $C_j = 1$. The first one is stable and describes the state where all clocks are set to a value larger than j; the second one is unstable and corresponds to the case where all clocks are set to values less than j. As time proceeds, all clock values are continuously increased, and hence in the context of this model it is natural to consider the invasion of the unstable state $C_j = 1$ by the stable state $C_j = 0$ [24]. Our main result for such type of fronts can be stated as follows.

We consider initial conditions such that there exists a $\lambda_0 > \lambda^*$ with λ^* given in (1.9) below, such that

$$0 \leqslant C_j(0) \leqslant 1 \quad \text{for all } j \quad \text{and} \quad \lim_{j \to \infty} [1 - C_j(0)] \, e^{\lambda_0 j} = 0. \tag{1.6}$$

We will refer to these initial conditions as 'sufficiently steep' [6]. Unlike for the differential equation (1.1), there are no continuous level curves for difference equations, but only discrete points in the (i, t) space where a certain level is reached; it is therefore most convenient to define the front position $x_f(t)$ in our case as

$$x_f(t) = \sum_{j=0}^{\infty} [1 - C_j(t)]. \tag{1.7}$$

The central result of this paper is that for initial values which satisfy (1.6), the front velocity $v(t) = \dot{x}_f(t)$ is asymptotically given by

$$v(t) = v^* + \dot{X}(t),$$
$$\dot{X}(t) = -\frac{3}{2\lambda^* t} \left(1 - \frac{\sqrt{\pi}}{\lambda^* \sqrt{Dt}} \right) + \mathcal{O}\left(\frac{1}{t^2}\right), \qquad t \to \infty. \tag{1.8}$$

Here λ^* is the solution of

$$2e^{\lambda^*} = \frac{2e^{\lambda^*} - 1}{\lambda^*} \quad \Rightarrow \quad \lambda^* = 0.768039, \tag{1.9}$$

and

$$v^* = \frac{2e^{\lambda^*} - 1}{\lambda^*} = 4.31107, \qquad D = e^{\lambda^*} = 2.155535. \tag{1.10}$$

Note that the $1/t$ power law relaxation of the velocity correction $\dot{X}(t)$ implies an unbounded logarithmic shift $X(t) \sim \ln t$ in the position of the front. We shall illustrate the importance of this logarithmic shift in Figure 1.

The asymptotic expression for $v(t)$ presented in (1.8) is exactly the same as the expression that was recently derived by Ebert & van Saarloos [6, 5] for the velocity relaxation in (1.1) and in higher order evolution equations that admit uniformly translating pulled fronts; for (1.1) one simply has $\lambda^* = 1$, $D = 1$ and $v^* = 2$. (The leading order correction $v(t) = 2 - 3/(2t)$ for Eq. (1.1) first was derived in [3].)

Thus, while the behavior of kinks or fronts between two (meta)stable states can change drastically when the nonlinear diffusion equation is replaced by a finite difference

approximation (one possibility being propagation failure [12, 7, 4, 25, 26]), the dynamical mechanism that leads to pulled fronts is completely the same in both types of equations. In fact, by a combination of analytical and numerical methods, two of us [6] have argued that (1.8) holds for all equations that admit uniformly translating pulled fronts. The parameters v^*, λ^* and D in (1.8) can generally be expressed in terms of the dispersion relation $\omega(k)$ of the evolution equation linearized about the unstable state. We refer to Ebert & van Saarloos [6] for an extensive discussion of this connection, and of the derivation of the explicit expressions.

In our view, the common features of pulled fronts expressed by (1.8) suggest that many of the methods developed in the mathematical literature for (1.1) (e.g. [8, 13, 2, 15, 9, 10]) may be generalized to much larger classes of equations. The present paper provides a first step in this direction, in that we explicitly confirm that for equation (1.2), a number of elements of the analysis of Ebert & van Saarloos [6] can be made mathematically more precise or be proven.

2 Derivation of the main results

We now turn to the derivation of these results for equation (1.2). We shall do this through the series of steps (i)–(vii). To facilitate the comparison with (1.1), we first transform to the variables $\phi_j = 1 - C_j$. In these, the dynamical equation reads

$$d\phi_j/dt = 2\phi_{j-1} - \phi_j - \phi_{j-1}^2, \tag{2.1}$$

and the initial condition (1.6) becomes

$$0 \leqslant \phi_j(0) \leqslant 1 \quad \text{for all } j, \quad \text{and} \quad \lim_{j \to \infty} \phi_j(0)\, e^{\lambda_0 j} = 0 \quad \text{for some} \quad \lambda_0 > \lambda^*. \tag{2.2}$$

The invaded unstable state is now $\phi_j \equiv 0$ and the invading state is $\phi_j \equiv 1$. From (1.2) and (1.6), we see that $C_j(t) \geqslant 0$, so that $\phi_j(t) \leqslant 1$ for all j and $t \geqslant 0$, and an elementary comparison argument shows that $\phi_j(t) \geqslant 0$ for all j and $t \geqslant 0$. Thus

$$0 \leqslant \phi_j(t) \leqslant 1 \quad \text{for} \quad j \in \mathbf{Z}, \ t \geqslant 0. \tag{2.3}$$

(i) *Instability and dispersion relation*
That the state $\phi_j = 0$ is unstable, can easily be seen as follows. We linearize the dynamical equation about $\phi = 0$ to get

$$d\phi_j/dt = 2\phi_{j-1} - \phi_j \tag{2.4}$$

and substitute a Fourier mode $\phi(x, t) = Ae^{-i(\omega t - kj)}$ with k in the 'Brillouin zone' $-\pi < k \leqslant \pi$. This yields the dispersion relation

$$-i\omega(k) = 2e^{-ik} - 1. \tag{2.5}$$

As the growth rate is given by $\text{Re}(-i\omega) = \text{Im}\,\omega = 2\cos k - 1$, modes with $|k| < \pi/3$ grow in time, so that the state $\phi = 0$ is unstable.

(ii) *Nonlinear versus linear dynamics*
For a given initial condition $\phi_j(0)$, the dynamics resulting from the linear equation (2.4) is an upper bound for the dynamics resulting from the nonlinear equation (2.1). To see

this, suppose that ϕ_j is the solution of the nonlinear equation and $\hat{\phi}_j$ the solution of the linear equation, and that ϕ_j and $\hat{\phi}_j$ have the same initial values. Then the difference $z_j = \hat{\phi}_j - \phi_j$ satisfies the equation

$$dz_j/dt = 2z_{j-1} - z_j + \phi_{j-1}^2, \qquad z_j(0) = 0. \tag{2.6}$$

Because the inhomogeneous term ϕ_{j-1}^2 is non-negative, it follows from standard theory [11] that $z_j(t) \geqslant 0$, and hence that $\phi_j(t) \leqslant \hat{\phi}_j(t)$ for all j and all $t \geqslant 0$. Thus solutions of the linear equation provide an upper bound to solutions of the nonlinear equation.

(iii) v^* *as upper bound for sufficiently steep initial conditions*
We now introduce the family of comparison functions

$$\eta_j(t; \lambda, v) = e^{-\lambda(j - vt)}, \qquad \lambda \in \mathbf{R}^+, \tag{2.7}$$

Substitution shows that η_j is a solution of the linear equation (2.4) if λ and v are related by

$$v = v(\lambda) = \frac{2e^\lambda - 1}{\lambda}. \tag{2.8}$$

We choose λ such that the speed $v(\lambda)$ defined by (2.8) takes on its smallest possible value. This is the case for $\lambda = \lambda^*$, as defined in (1.9). The corresponding velocity is denoted by v^*. Then, for any $A > 0$, we have

$$\phi_j(t) \leqslant Ae^{-\lambda^*(j - v^*t)} \quad \text{if} \quad \phi_j(0) \leqslant Ae^{-\lambda^* j} \quad \text{for all} \quad j. \tag{2.9}$$

Thus, for initial data which decay sufficiently fast as defined by (2.2), the nonlinearity in (2.1) cannot push the front in the large time limit to a velocity higher than v^*, which is determined by the linear equation. Rather, the leading edge, i.e. the region defined through $\phi_j \approx 0$, will 'pull' the front along: since the nonlinear term only decreases the growth, the nonlinear region is 'pulled' along by the growth and spreading of the leading edge into the unstable state. The dynamics of the leading edge is described by the linearized equations. Indeed, one may show quite generally by means of a long time asymptotic analysis of the Green function of the equations linearized about the unstable state, that v^* is nothing but the asymptotic linear spreading velocity [14, 6]. This creates the particular mode of pulled front propagation, that is unlike the nonlinear mechanisms dominating pushed and bistable fronts – as we shall illustrate in the concluding section, for such fronts the nonlinearities enhance the growth so much that they start to dominate the dynamics.

The upper bound (2.9) is not strong enough for our subsequent analysis. Using a comparison function with decay rate $\lambda = \lambda_0 > \lambda^*$ that bounds the initial data (2.2), it follows immediately that for every fixed and finite $t \in \mathbf{R}^+$, the sequence $\phi_j(t)$ can also be bounded by

$$\phi_j(t) \leqslant A \, e^{\lambda_0 v(\lambda_0) t} \cdot e^{-\lambda_0 j} \quad \text{for } \lambda_0 > \lambda^*. \tag{2.10}$$

Thus, for any fixed time t, the solution $\phi_j(t)$ is exponentially bounded for $j \to \infty$.

(iv) *Leading edge representation*
Let us now turn to the systematic calculation of the wave speed. To understand the convergence towards an asymptotic nonlinear front profile in the pulled regime, we introduce, what has been called the *leading edge representation* ψ [6]. This involves the
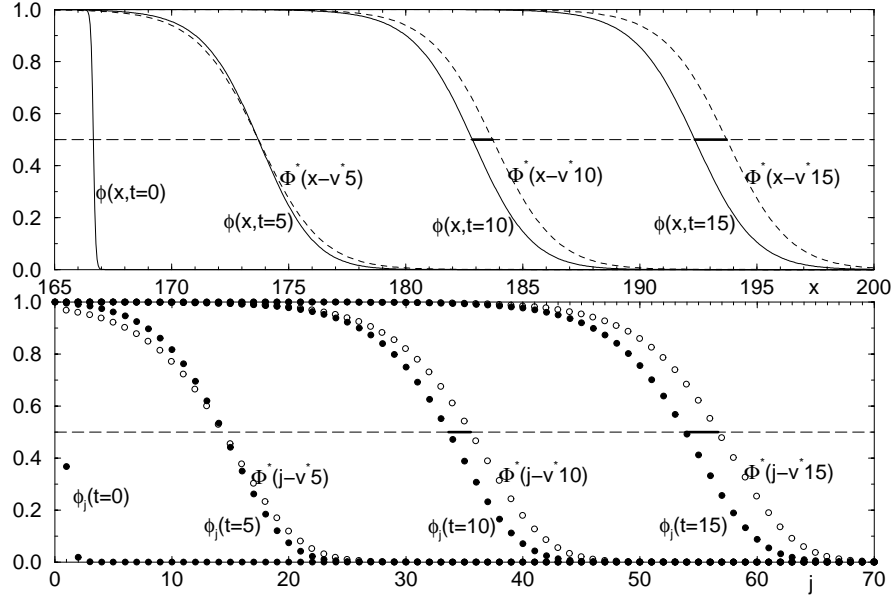
FIGURE 1. Illustration of the fact, that even though the shape of a front profile is quite close to the asymptotic one, its position is shifted logarithmically in time relative to the uniformly translating profile Φ^*, since $X(t)$ increases as $\ln(t)$ for large times. Upper panel: numerical solution of the nonlinear diffusion equation (1.1) with $f(\phi) = \phi - \phi^3$. Solid lines: evolution of some initial condition of the form $\phi(x,0) = 1/\left[1 + e^{10(x-x_0)}\right]$ at times $t = 0, 5, 10, 15$. Dashed lines: $\Phi^*(x - v^*t)$ at times $t = 5, 10, 15$. The initial position of Φ^* is chosen in such a way that the amplitude $\Phi^* = 1/2$ coincides with $\phi(x,t) = 1/2$ at time $t = 5$. The logarithmic temporal shift is indicated by the fat line. Lower panel: numerical solution of the difference-differential equation (2.1), starting from initial conditions (3.1). The open circles indicate the asymptotic uniformly translating solution, while the solid dots indicate the actual solution at time $t = 0, 5, 10$ and 15. Note that apart from a different spatial scale on the horizontal axis, associated with the fact that v^* and λ^* are different for the two equations, the two plots are very similar in appearance. The plots also illustrate the fact that any analysis based on linearizing about the uniformly translating asymptotic front solution Φ^* will break down, since the distance between the actual solution and Φ^* diverges in time.

transformation to a coordinate frame $\xi_X = x - v^*t - X(t)$ which moves with a speed $v^* + \dot{X}(t)$. Thus $X(t)$ is a – as yet undetermined – time-dependent shift. Following the asymptotic analysis of the Green function of the linearized equation (2.4) (see Ebert & van Saarloos [6]), one is led to make the Ansatz that $\dot{X}(t) = c_1/t + \mathcal{O}(1/t^{3/2})$ as $t \to \infty$, where $c_1 < 0$. Plainly then,

$$X(t) = \int_0^t \{v(s) - v^*\}\, ds \approx c_1 \ln t \to -\infty \quad \text{as} \quad t \to \infty. \tag{2.11}$$

The importance of using the logarithmically shifted time frame ξ_X for calculating the long-time asymptotic behavior of pulled fronts is illustrated in Figure 1 for both the nonlinear diffusion equation (1.1) and our difference-differential equation. The solid lines or solid dots, respectively, show different steps of the temporal evolution of a front, that has started from a sufficiently steep initial condition. The dashed lines or open circles,

respectively, are the asymptotic uniformly translating front solutions $\Phi^*(x - v^*t)$ with $v^* = 2$ for the nonlinear diffusion equation (1.1) and similarly $\Phi^*(i - v^*t)$ with v^* given by (1.10) for the difference-differential equation (2.1); the latter was obtained numerically from a long time integration. As the data show, the actual front shape $\phi(x, t)$ is quite similar to Φ^* for times $t \geqslant 5$, but as the fat solid line illustrates, the distance between the actual transient front $\phi(x, t)$ and the uniformly translating solution $\Phi^*(x - v^*t)$ increases without bound, in accordance with (2.11). The similarity of the two plots for both our difference-differential equation and the nonlinear diffusion equation (1.1) suggests that the same logarithmic shift occurs in both equations, and thus illustrates that the underlying mechanism is the same for both of them and in fact, according to Ebert & van Saarloos [6], for any pulled front.

In addition to the moving frame ξ_X, we introduce an exponential factor $e^{-\lambda^* \xi_X}$ that is motivated by (2.9). Thus, we put

$$\phi_j(t) = e^{-\lambda^* \xi_X} \, \psi(\xi_X, t), \quad \xi_X = j - v^*t - X(t). \tag{2.12}$$

Of course, at any fixed time t, the variable ξ_X is only defined at discrete points, whose position varies linearly with t. However, the transformation from $\phi_j(t)$ to $\psi(\xi_X, t)$ in (2.12) anticipates that for large t and ξ_X, the solution $\psi(\xi_X, t)$ will be arbitrarily slowly varying in time and space, so that discretization effects become unimportant. Transforming equation (2.1) for $\phi_j(t)$ into an equation for $\psi(\xi_X, t)$, we find

$$\frac{\partial \psi(\xi_X, t)}{\partial t} = v^* \left[\psi(\xi_X - 1, t) - \psi(\xi_X, t) + \frac{\partial \psi(\xi_X, t)}{\partial \xi_X} \right] \tag{2.13}$$
$$+ \dot{X}(t) \left[\frac{\partial}{\partial \xi_X} - \lambda^* \right] \psi(\xi_X, t) - \frac{v^*}{2} \, e^{-\lambda^*(\xi_X - 1)} \, \psi(\xi_X - 1, t)^2.$$

In deriving (2.13), we divided out a common factor $e^{-\lambda^* \xi_X}$, and used the identities (1.9) and (1.10) for v^* and λ^*. The idea is now to determine $X(t)$ such that $\psi(\xi_X, t)$ converges to a time independent limit $\Psi(\xi_X)$ as $t \to \infty$, i.e.

$$|\psi(\xi_X, t) - \Psi(\xi_X)| \to 0 \quad \text{as} \quad t \to \infty, \tag{2.14}$$

uniformly on intervals of the form $(-\infty, L]$, for any $L \in \mathbf{R}$. We shall refer to $\psi(\xi_X)$ as the *asymptotic front shape*. In Figure 1, we already illustrated that the convergence (2.14) occurs only in the properly shifted frame ξ_X, both for the partial differential equation (1.1) and for the difference-differential equation (2.1).

(v) *The asymptotic shape of the leading edge*

The profile $\Psi(\xi)$ in the long time asymptotics is the solution of the equation

$$\Psi(\xi - 1) - \Psi(\xi) + \Psi'(\xi) = \frac{1}{2} \, e^{-\lambda^*(\xi - 1)} \, \Psi^2(\xi - 1), \tag{2.15}$$

which we have obtained from (2.13) by suppressing the t-dependence, and setting $\dot{X}(t) = 0$. In the leading edge transformation (2.12) we divided out the dominant exponentially decaying factor. Therefore, the relevant function $\Psi(\xi)$ can diverge at most algebraically to infinity, so that the right-hand side of (2.15) decays exponentially as $\xi \to \infty$. Hence, by

an elementary argument involving the Laplace transform, $\Psi(\xi)$ behaves asymptotically as[1]

$$\Psi(\xi) \sim \alpha\xi + \beta \quad \text{as} \quad \xi \to \infty \quad (\alpha, \beta \in \mathbf{R}). \tag{2.16}$$

Since ϕ_j approaches 1 behind the front, the transformation (2.12) implies that

$$\Psi(\xi) = \mathcal{O}\left(e^{\lambda^* \xi}\right) \quad \text{as} \quad \xi \to -\infty. \tag{2.17}$$

By integrating (2.15) over $(-\infty, b)$, letting $b \to \infty$ and using (2.16) and (2.17) we obtain

$$\alpha = \int_{-\infty}^{\infty} e^{-\lambda^* \xi} \, \Psi^2(\xi) \, d\xi > 0. \tag{2.18}$$

The fact that α is positive stems from the nonlinearity in the equation as is clear from equation (2.18). This is why the linearized equation fails to give the correct long time convergence of the solution, even though the linear spreading velocity v^* is a property of the linear equations. This point is further elaborated in § 2.5.1 and § 3.1.1 of Ebert & van Saarloos [6].

(vi) *The spatial decay of the evolving front*
The initial condition (2.2) implies that $\psi(\xi_X, 0) \to 0$ as $\xi_X \to \infty$. Equation (2.10) shows that this stays true for any fixed and finite time $t > 0$, since

$$\psi(\xi_X, t) \leqslant A(t) \cdot e^{-\delta \, \xi_X}, \qquad A(t) = A \, e^{\lambda_0 \left[v(\lambda_0)t - v^* t - X(t)\right]} \tag{2.19}$$
$$\text{for} \quad \xi_X \to \infty \quad \text{and fixed} \ t \in \mathbf{R}^+ \quad \text{and} \quad \delta = \lambda_0 - \lambda^* > 0.$$

On the other hand, for any fixed $\xi_X \gg 1$, (2.14) together with (2.16) gives

$$\psi(\xi_X, t) = \alpha\xi_X + \beta \quad \text{for} \ \ t \to \infty \ \ \text{and fixed} \ \ 1 \ll \xi_X < \infty, \tag{2.20}$$

if we make the appropriate choice for $X(t)$. Note that according to (2.19) the large ξ_X limit of ψ vanishes for any finite time, while in the infinite time limit ψ diverges linearly in ξ_X. This illustrates that the limits $t \to \infty$ and $\xi_X \to \infty$ do not commute. The divergence of the linear growth in the limit of (2.20) for $t \to \infty$ illustrates the buildup in the intermediate asymptotic region.

(vii) *The rate of convergence*
We now determine the large time asymptotics of $X(t)$ from the solution of equation (2.13) with limiting conditions (2.19) and (2.20). For large ξ_X, the nonlinearity in (2.13) can be neglected, since $e^{-\lambda^* \xi_X} \psi^2 \ll \psi$ because of (2.19) and $e^{-\lambda^* \xi_X} \ll 1$. Anticipating that also the higher order derivatives become small for large values of ξ_X, we expand $\psi(\xi_X - 1)$ at ξ_X:

$$\psi(\xi_X - 1, t) = \psi(\xi_X, t) - \partial_{\xi_X}\psi(\xi_X, t) + \frac{1}{2}\partial_{\xi_X}^2\psi(\xi_X, t) - \frac{1}{3!}\partial_{\xi_X}^3\psi(\xi_X, t) + \dots. \tag{2.21}$$

Explicit solutions of the time-dependent linearized equation show that this expansion is justified for sufficiently large values of t, when ψ approaches the smooth function

---

[1] Another argument, that leads to the same conclusion is to transform equation (2.15) back to the ϕ variable, which yields $\Phi^*(\xi) - v^* \partial_\xi \Phi^*(\xi) = 2\Phi^*(\xi - 1) - \Phi^{*2}(\xi - 1)$. By investigating the flow near the fixed points $\Phi = 1$ and $\Phi = 0$, such a front can be shown directly to decay towards $\xi \to \infty$ as $\Phi^*(\xi) = (\alpha\xi + \beta) \, e^{-\lambda^* \xi}$. For Ψ this implies the behavior given in (2.16).

$\Psi(\xi_X) = \alpha\xi_X + \beta$. When we substitute this expansion into equation (2.13), we obtain

$$\partial_t\,\psi = D\,\partial^2_{\xi_X}\psi + D_3\,\partial^3_{\xi_X}\psi + \ldots + \dot{X}(t)\Big[\partial_{\xi_X} - \lambda^*\Big]\psi, \tag{2.22}$$

where the function ψ is now everywhere evaluated at (ξ_X, t), and $D_n = (-1)^n v^*/n!$ with $D = D_2$. If we were to set $\dot{X} = 0$, and omit the derivatives of order three and higher, we would obtain the classical diffusion equation. This motivates the use of the Gaussian similarity variable

$$z = \frac{\xi_X^2}{4Dt} \tag{2.23}$$

as a substitution for ξ_X. For $X(t)$ we anticipate an expansion of the type

$$\dot{X}(t) = \frac{c_1}{t} + \frac{c_{3/2}}{t^{3/2}} + \frac{c_2}{t^2} + \cdots, \tag{2.24}$$

where the leading order $1/t$ is consistent with (2.11), and the further expansion in powers of $1/\sqrt{t}$ is motivated by the substitution of ξ_X by z. For ψ in the region $\xi_X \leqslant \mathcal{O}(\sqrt{t})$, we make an Ansatz with the same structure,

$$\psi(\xi_X, t) = \Psi(\xi_X) + \frac{\psi_1(\xi_X)}{t} + \frac{\psi_{3/2}(\xi_X)}{t^{3/2}} + \ldots \quad \text{for } \xi_X \leqslant \mathcal{O}(\sqrt{t}). \tag{2.25}$$

Note that a term of order $1/t^{1/2}$ is absent here. This can be understood from the fact that the use of a time-dependent frame shifted by $X(t)$ introduces correction terms proportional to $v(t) - v^* = \dot{X}(t)$, which in dominant order goes as t^{-1}; it can also be derived more formally from a resummation of the terms in the interior region of the front, as discussed in Ebert & van Saarloos [6].

In the region $\xi_X \geqslant \mathcal{O}(\sqrt{t})$, we make the Ansatz

$$\psi(\xi_X, t) = e^{-z}\left[\sqrt{t}\,g_{-1/2}(z) + g_0(z) + \frac{g_{1/2}(z)}{\sqrt{t}} + \ldots\right] \quad \text{for } \xi_X \geqslant \mathcal{O}(\sqrt{t}), \tag{2.26}$$

where we have used (2.23) to write the right-hand side in terms of z and t. Here a Gaussian e^{-z} is already factorized out for later convenience. By asymptotic matching, equations (2.20) and (2.25) determine the small z expansion of the functions g for $z \downarrow 0$ as

$$g_{-1/2}(z) = 2\alpha\sqrt{z} + \mathcal{O}\left(z^{3/2}\right), \tag{2.27}$$

$$g_0(z) = \beta + \mathcal{O}(z). \tag{2.28}$$

The limit as $z \to \infty$ for fixed $t < \infty$ is determined by (2.19) as

$$g_{-1/2}(z) \leqslant A(t)\,t^{-1/2}\,e^z\,e^{-\delta\sqrt{4Dt}\,\sqrt{z}}\,, \quad g_0(z) \leqslant A(t)\,e^z\,e^{-\delta\sqrt{4Dt}\,\sqrt{z}}. \tag{2.29}$$

The functions $g_{-1/2}(z)$, $g_0(z)$ and $g_{1/2}(z)$ satisfy linear differential equations which we obtain by equating the coefficients of $t^{1/2}$, t^0 and $t^{-1/2}$ to zero. For $g_{-1/2}(z)$ this yields the equation

$$zg'' + \left(\frac{1}{2} - z\right)g' - (1 + c_1\lambda^*)g = 0 \tag{2.30}$$

and for g_0 we obtain

$$zg'' + \left(\frac{1}{2} - z\right)g' - \left(\frac{1}{2} + c_1\lambda^*\right)g = h(z), \tag{2.31}$$

where

$$h(z) = e^z \left[c_{3/2} \lambda^* - \frac{c_1}{\sqrt{D}} \sqrt{z} \frac{d}{dz} - \frac{D_3 \sqrt{z}}{D^{3/2}} \left(\frac{3}{2} \frac{d^2}{dz^2} + z \frac{d^3}{dz^3} \right) \right] e^{-z} g_{-1/2}(z). \tag{2.32}$$

The general solutions of the homogeneous differential equations are confluent hypergeometric functions $M(a, b, z)$, for which we use the notation of Abramowitz & Stegun [1].

Equation (2.30) only has a solution obeying the boundary conditions (2.27) and (2.29), if $-c_1 \lambda^* - 1/2$ is a positive integer [1, 6]. In this case, the solution is

$$g_{-1/2}(z) = 2\alpha \sqrt{z} \, M \left(c_1 \lambda^* + \frac{3}{2}, \frac{3}{2}, z \right), \tag{2.33}$$

which can be identified with a Hermite polynomial. The relevant solution is

$$c_1 \lambda^* = -3/2, \quad \text{so that} \quad g_{-1/2}(z) = 2\alpha \sqrt{z}, \tag{2.34}$$

since it is the only solution consistent with the conserved positivity (2.3) of the solution.

A particular solution of the inhomogeneous equation (2.31) for $g_0(z)$ with inhomogeneity $h(z)$ given by (2.32) and (2.34) has been constructed in [6]. We there find that a construction of the full solution of (2.31) with boundary conditions (2.28) and (2.29) is only possible, if

$$c_{3/2} \lambda^* = -\sqrt{\pi} \frac{c_1}{\sqrt{D}}. \tag{2.35}$$

Note, that the coefficient D_3 of the third spatial derivative in (2.22) enters (2.32), but does not influence $c_{3/2}$. It does give a contribution to $g_0(z)$, however, whose explicit analytical form can be found in Ebert & van Saarloos [6].

Equations (2.24), (2.34) and (2.35) yield our explicit prediction (1.8) for the velocity of the evolving front $v(t) = v^* + \dot{X}(t)$.

3 Numerical verification

In Figure 2 we show numerical data for the front velocity, obtained by numerically solving equation (1.2) [or (2.1) after the transformation $\phi_j(t) = 1 - C_j(t)$] with initial condition

$$\phi_j(0) = \begin{cases} e^{-j^2} & \text{for } j \geqslant 0 \\ 1 & \text{for } j < 0, \end{cases} \tag{3.1}$$

which is a sufficiently steep initial condition according to the definition (2.2). The front velocity is defined in (1.7) as $v(t) = \dot{x}_f(t) = \sum_{j=0}^{\infty} \dot{\phi}_j(t)$. To bring out that all terms up to order $t^{-3/2}$ in our expansion are fully corroborated by our numerical simulations, we plot in Figure 2 the expression

$$\left[v(t) - v^* + \frac{3}{2\lambda^* t} \right] t^{3/2} \tag{3.2}$$

versus $1/\sqrt{t}$. According to our analysis, this expression should approach the value

$$3/(2\lambda^{*2}) \sqrt{\pi/D} = 3.06989 \quad \text{as} \quad t \to \infty.$$

This value is indicated with a cross in Figure 2. Note that at the latest time $t = 4000$, $t^{3/2} = 2.5 \cdot 10^5$, so an error in the sixth decimal place in any of our terms for $v(t)$ would be clearly visible in the figure. The fact that our numerical data approach our analytical value so well, thus confirms our analytical results with extreme precision.
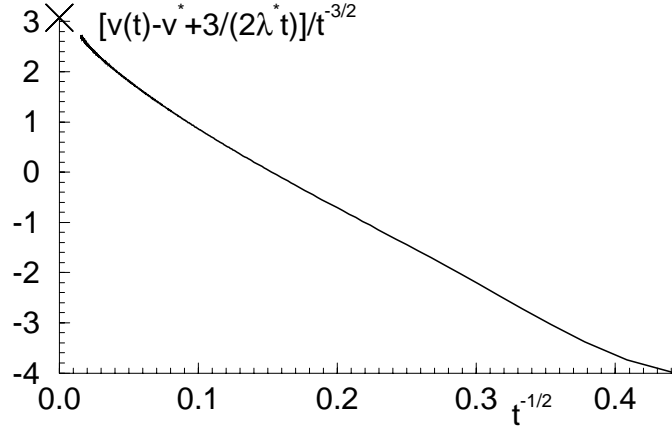
FIGURE 2. Numerical solution of (1.2) with initial conditions (3.1). The velocity $v(t) = \dot{x}_f(t)$ of the front is defined in (1.7). Plotted is $(v(t) - v^* - c_1/t)/t^{-3/2}$ as a function of $1/\sqrt{t}$ for times $40 \leqslant t \leqslant 4000$. $c_{3/2}$ is marked by the cross on the axis. The constants are $c_1 = -3/(2\lambda^*)$ (2.34) and $c_{3/2} = -\sqrt{\pi/D}\, c_1/\lambda^*$ (2.35) with λ^*, v^*, and D from (1.9) and (1.10). The analytical prediction (1.8) implies that the curve should extrapolate approximately linearly towards the cross. Clearly, the numerics fully confirms this prediction.

4 Conclusion and outlook

We finally note that the prediction (1.8) for the velocity $v(t)$ of an evolving pulled front is a 'universal' result:

(a) It is independent of the precise initial conditions provided they obey the bound (2.2).
(b) It is independent of the precise nonlinearities, provided they create pulled fronts, where the concept of pulling is explained in (i)–(iv). A different nonlinearity will only affect the value of α in (2.16), but as long as $\alpha > 0$, the velocity converges to its asymptotic value v^* according to (1.8).
(c) In the introduction, we already mentioned that the result (1.8) also holds for the nonlinear diffusion equation (1.1) with the parameters v^*, λ^* and D depending on the equation through the explicit expressions in terms of the dispersion relation of the unstable mode (e.g. see (1.4) and (1.5) of Ebert & van Saarloos [6]). As has been stated earlier, the asymptotic expression (1.8) for $v(t)$ likewise holds more generally for all equations that for $t \to \infty$ generate uniformly translating pulled fronts [6]. The generalization to pulled fronts that generate patterns (such as in the Swift-Hohenberg equation) can be found in Storm *et al.* [19]. Thus, the line of reasoning on which the analysis is built can be viewed as evidence that there is a center manifold governing the convergence of pulled fronts in general.
(d) In this paper, we have focused on the results for the convergence of the velocity associated with the front position $x_f(t)$ defined in (1.7). We can actually go much further and analyze the convergence of the front profile as well. Indeed, if we denote with $\Phi_v(\xi)$ the uniformly translating front profile with velocity v, one may show along the lines of Ebert & van Saarloos [6] that $\phi_j(t) = \Phi_{v(t)}(\xi_X) + O(1/t^2)$. This result implies that the velocity $v_\phi(t)$ of a given level $\phi_j(t) = \phi$ is independent of the value of ϕ within

the accuracy given in (1.8). Therefore also the definition of the front velocity through (1.7) invariably results in the same prediction (1.8).

As we stressed in the introduction, our dynamical equation is very asymmetric, in that the dynamics at site j depends only on the variables at sites j and $j-1$. Indeed, fronts connecting the stable state to the unstable state to the left of it (into the negative j direction), have a very different speed: they actually recede, i.e. propagate into the *positive* j direction, not in the *negative* j direction. Nevertheless, their dynamics is governed by exactly the same mechanism: their asymptotic speed is the spreading speed $v_2^* = 0.3734$ associated with the negative lambda solution $\lambda_2^* = -1.678$ of (1.9). Likewise, there is again a power law relaxation given by equation (1.8) with appropriate values of λ^* and D.

The equation we have studied is an example of an equation whose relevant dynamics is 'pulled', i.e. whose front solutions asymptotically approach the linear spreading speed v^*. As is well known, for the nonlinear diffusion equation (1.1) fronts can also be 'pushed' depending on the nonlinearities of $f(\phi)$. The *o.d.e.*-solutions associated with such front solutions are "strongly heteroclinic orbits" [17], orbits which flow into the fixed point corresponding to the unstable state along the eigendirection whose contraction is not the slowest but the second slowest. Experience with various equations (extensions of the Swift-Hohenberg equation [22], the complex Ginzburg-Landau equation [23], coupled amplitude equations [21], stochastic lattice models [20]) lead one to believe that also the strongly heteroclinic orbit scenario leading to pushed fronts is found in more general classes of equations, like the differential-difference equation studied here. Although there is no general criterion for the transition from the pulled to the pushed regime, as a general rule one has pulled fronts when all nonlinearities are saturating – as one has indeed in (2.1) – while one expects pushed fronts when the nonlinearity initially enhances the growth before the saturation sets in. Indeed, if we add to (2.1) a term so that it becomes

$$d\phi_j/dt = 2\phi_{j-1} - \phi_j - \phi_{j-1}^2 + \mu\phi_{j-1}^2(1 - \phi_{j-1}), \qquad (4.1)$$

then we expect that for sufficiently large values of μ one will get a transition to the pushed regime. This is confirmed by numerical studies. By extracting the asymptotic speed of front solutions emerging from initial conditions (3.1), we have found that the critical value μ_c is 0.544 ± 0.002, and that for $\mu \geqslant \mu_c$ one has $v \approx v^* + 1.43(\mu - \mu_c)^2 + \ldots$. Typically, the stability spectrum of pushed front solutions is gapped, and the relaxation towards the pushed front solution is exponential [6].

In our view, this universality of pulled front propagation in both the nonlinear diffusion equation (1.1) and in the difference-differential equation (1.2) and in other dynamical equations [6, 19] is an indication that many of the methods developed in the mathematical literature [8, 13, 2] for equation (1.1) should be generalizable to much larger classes of equations like higher order partial differential equations, difference equations, integro-differential equations, sets of coupled equations etc.

Acknowledgements

References

[1] ABRAMOWITZ, M. & STEGUN, I. S. (EDITORS) (1972) *Handbook of Mathematical Functions*. Dover.

[2] ARONSON, D. G. & WEINBERGER, H. F. (1978) Multidimensional nonlinear diffusion arising in population genetics. *Adv. Math.* **30**, 33.

[3] BRAMSON, M. (1983) Convergence of solutions of the Kolmogorov equation to travelling waves. *Mem. Am. Math. Soc.* **44**(285).

[4] CARPIO, A., CHAPMAN, S. J., HASTINGS, S. P. & McLEOD, J. B. (2000) Wave solutions for a discrete reaction-diffucion equation. *Euro. J. Appl. Math.* **11**, 399–412.

[5] EBERT, U. & VAN SAARLOOS, W. (1998) Universal algebraic relaxation of fronts propagating into an unstable state and implications for moving boundary approximations. *Phys. Rev. Lett.* **80**, 1650–1653.

[6] EBERT, U. & VAN SAARLOOS, W. (2000) Fronts propagating uniformly into unstable states: Universal algebraic convergence of pulled fronts. *Physica D* **146**, 1–99.

[7] FÁTH, G. (1998) Propagation failure of traveling waves in a discrete bistable medium. *Physica D* **116**, 176.

[8] FISHER, R. A. (1937) The wave of advance of advantageous genes. *Ann. Eugenics*, **7**, 355.

[9] GALLAY, TH. & RAUGEL, G. (2000) Stability of propagating fronts in damped hyperbolic equations. In: Jäger, W., Neǎs, J., John, O., Najzar, K. and Stará, J. (editors), *Partial Differential Equations: Theory and numerical solutions*, Chapman & Hall Research Notes in Mathematics 406, 130–146.

[10] GALLAY, TH. & RAUGEL, G. (2000) Scaling variables and stability of hyperbolic fronts. *SIAM J. Math. Anal.* **32**, 1–29.

[11] HIRSCH, M. W. (1982) Systems of differential equations which are competetive or cooperative. I: limit sets. *SIAM J. Math. Anal.* **13**, 167–179.

[12] KEENER, J. P. (1987) Propagation and its failure in coupled systems of discrete cells. *SIAM J. Appl. Math.* **47**, 556.

[13] KOLMOGOROFF, A., PETROVSKY, I. & PISCOUNOFF, N. (1937) Study of the diffusion equation with growth of the quantity of matter and its application to a biology problem. *Bull. Univ. Moscou*, Ser. Int., sec. A, Vol. 1 (translated and reprinted in Pelcé, P., *Dynamics of Curved Fronts*, (Academic Press, San Diego, 1988).

[14] LANDAU, L. D. & LIFSHITZ, E. M. (1981) *Course of Theoretical Physics*, vol. 10: *Physical Kinetics*. Pergamon.

[15] OGIWARA, T. & MATANO, H. (1999) Monotonicity and convergence results in order-preserving systems in the presence of symmetry. *Discr. Cont. Dyn. Syst.* **5**, 1–34.

[16] PAQUETTE, G. C., CHEN, L.-Y., GOLDENFELD, N. & OONO, Y. (1994) Structural stability and renormalization group for propagating fronts. *Phys. Rev. Lett.* **72**, 76–79.

[17] POWELL J. A., NEWELL A. C. & JONES C. K. R. T. (1991) Competition between generic and nongeneric fronts in envelope equations. *Phys. Rev. A*, **44**, 3636–3652.

[18] STOKES, A. N. (1976) On two types of moving front in quasilinear diffusion. *Math. Biosci.* **31**, 307.

[19] STORM, C., SPRUIJT, W., EBERT, U. & VAN SAARLOOS, W. (2000) Universal algebraic relaxation of velocity and phase in pulled fronts generating periodic or chaotic states. *Phys. Rev. E*, **61**, R6063–R6066.

[20] TRIPATHY G. & VAN SAARLOOS W. (2000) Fluctuation and relaxation properties of pulled fronts: a possible scenario for non-KPZ-behavior. *Phys. Rev. Lett.* **85**, 3556–3559.

[21] TU Y. & CROSS M. C. (1999), Chaotic domain structure in rotating convection. *Phys. Rev. Lett.* **69**, 2515–2528.

[22] VAN SAARLOOS W. (1989) Front propagation into unstable states. II: Linear versus nonlinear marginal stability and rate of convergence. *Phys. Rev. A*, **39**, 6367–6390.

[23] VAN SAARLOOS W. & HOHENBERG P. C. (1992) Fronts, pulses, sources and sinks in generalized complex Ginzburg-Landau equations. *Physica D*, **56**, 303–367.

[24] VAN ZON, R., VAN BEIJEREN, H. & DELLAGO, CH. (1998) Largest Lyapunov exponent for many
      particle systems at low densities. *Phys. Rev. Lett.* **80**, 2035.
[25] ZINNER, B. (1991) Stability of traveling wave fronts for the discrete Nagumo equation. *SIAM
      J. Math. Anal.* **22**, 1016–1020.
[26] ZINNER, B. (1992) Existence of traveling wave front solutions for the discrete Nagumo equation.
      J. Diff. Eq. **96**, 1–27.